JOURNAL OF MAGNETIC RESONANCE, Series B 101, 114–119 (1993)

Correlation of Backbone Amide and Aliphatic Side-Chain Resonances in $^{13}C/^{15}N$-Enriched Proteins by Isotropic Mixing of ^{13}C Magnetization

STEPHAN GRZESIEK, JACOB ANGLISTER,* AND AD BAX

Laboratory of Chemical Physics, National Institutes of Diabetes and Digestive and Kidney Diseases, National Institutes of Health, Bethesda, Maryland 20892

Received October 26, 1992

A recently proposed experiment, known as CBCA(CO)NH, provides a sensitive and straightforward means for correlating the backbone amide $^1H/^{15}N$ resonances in a protein with the $^{13}C_\alpha$ and $^{13}C_\beta$ resonances of the preceding residue (*1*). This experiment, which relies on COSY-type magnetization transfer via the $^1J_{C\alpha C\beta}$ coupling, followed by magnetization relay from $^{13}C_\alpha$ via the carbonyl to the ^{15}N of the next residue, is applicable to uniformly $^{15}N/^{13}C$-enriched proteins with a size of up to 30 kDa. A slight modification of the experiment, known as HBHA(CBCACO)NH, permits correlation of the amide with the $^1H_\alpha$ and $^1H_\beta$ resonances of the preceding residue, and a detailed product-operator description of both experiments has been presented previously (*2*). Alternatively, using the CBCANH experiment (*3*), which uses magnetization transfer via the smaller $^1J_{NC\alpha}$ and $^2J_{NC\alpha}$ couplings, the backbone amide resonances can be correlated simultaneously with the intraresidue C_α/C_β resonances and with the C_α/C_β of the preceding residue. The sequential assignments for the backbone and C_β and H_β resonances then can be extended to the side-chain resonances using the HCCH–COSY (*4, 5*) and HCCH–TOCSY (*6, 7*) experiments, recorded on samples dissolved in D_2O.

Here we describe two 3D experiments, named H(CCO)NH and C(CO)NH, that can correlate all the aliphatic ^1H or ^{13}C resonances of a given amino acid directly with the amide of the next residue. The new methods are far more convenient for obtaining assignments than the previous combinations of H_2O and D_2O experiments as they provide a direct linkage between the backbone and entire side chains. This makes it possible to obtain nearly complete ^1H and ^{13}C assignments from only a few 3D spectra, recorded on a single sample, dissolved in H_2O.

Pulse schemes for the C(CO)NH and H(CCO)NH experiments are shown in Fig. 1. Conceptually, these experiments are quite similar to the CBCA(CO)NH and HBHA(CBCACO)NH experiments. The main difference is that the C(CO)NH and H(CCO)NH experiments use isotropic ^{13}C mixing instead of a 90° COSY-type pulse to transfer magnetization from the aliphatic side chain to C_α. Because the isotropic mixing period is followed by a relatively long dephasing delay, 2ζ, needed for the relay of C_α magnetization to the carbonyl (C′), analysis of the magnetization transfer is slightly more complex than that in the CBCA(CO)NH experiment, and below the magnetization-transfer steps in the C(CO)NH experiment will briefly be analyzed, with emphasis on the new features. The operators for the H_α, C_α, C_β, C′, N, and H_N spins are denoted H^α, C^α, C^β, C', N, and H^N, and for simplicity, the effects of relaxation are not taken into account. For the C_β methylene protons, they are denoted $H^{\beta 2}$ and $H^{\beta 3}$.

In the C(CO)NH experiment, depicted in Fig. 1A, the first step involves an INEPT transfer to enhance the nuclear spin magnetization of the aliphatic carbons. This INEPT transfer includes a spin-lock pulse which serves to scramble the water magnetization (*8*). After the INEPT transfer, at time point *c* in the sequence, ^{13}C magnetization is antiphase with respect to its directly attached proton. The subsequent ^{13}C refocusing and evolution period is improved relative to that in the HCCH–TOCSY experiment (*7*), where the t_1 evolution period follows a fixed delay needed for rephasing of the antiphase ^{13}C magnetization. In the present experiment, the rephasing delay is gradually incorporated into the t_1 frequency-labeling period as the t_1 interval increases (*2, 9*). This significantly enhances the resolution obtainable in the t_1 dimension. Consider, for example, methylene C_β magnetization at time point *c* for an amino acid which, for simplicity, is assumed not to contain an aliphatic C_γ. At time point *c*, the spin operator describing this magnetization is $2(C_y^\beta H_z^{\beta 2} + C_y^\beta H_z^{\beta 3})$. For symmetry reasons, the fate of only one of the two products needs to be analyzed.

* On leave from the Weizmann Institute, Rehovot, Israel.

1064-1866/93 $5.00

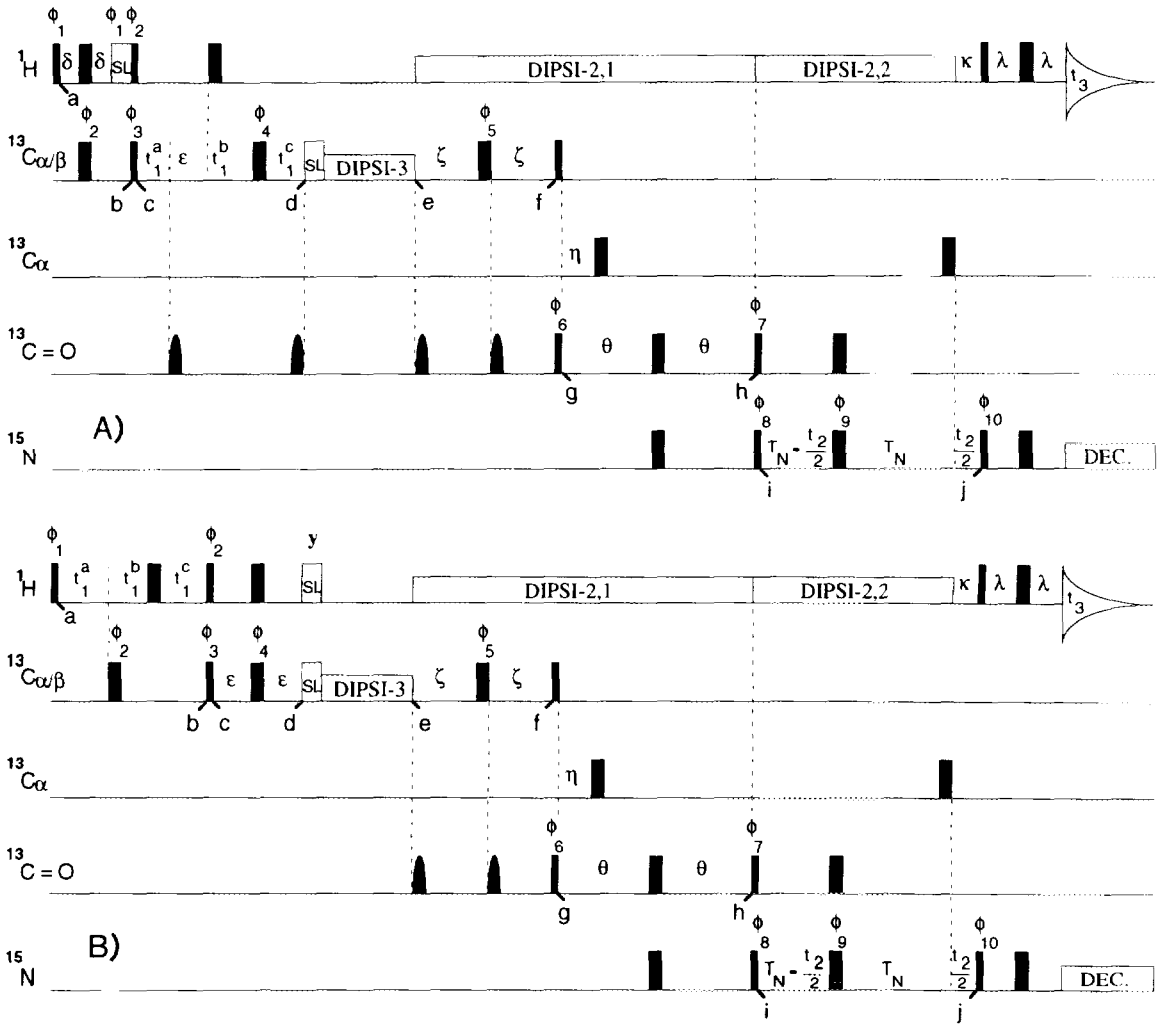

FIG. 1. Pulse scheme of (A) the C(CO)NH experiment and (B) the H(CCO)NH experiment. Narrow and wide pulses correspond to 90° and 180° flip angles, respectively. Pulses for which the phase is not indicated are applied along the x axis. The ^{1}H carrier is set to the H_2O frequency for the first part of the pulse sequence, up to time h, and is switched to the center of the amide region (8.4 ppm) thereafter. Thus, the frequency of the ^{1}H broadband decoupling (with a 5 kHz RF field) is switched at this point, and the two modes of decoupling, using a coherent DIPSI-2 scheme (*13*), are marked DIPSI-2,1 and DIPSI-2,2. ^{15}N decoupling is accomplished using WALTZ-16 modulation with a 1.5 kHz RF field. Carbonyl pulses have a shaped amplitude profile, corresponding to the center lobe of a sin x/x function and a duration of 202 μs. The carrier for the $C_{\alpha/\beta}$ pulses is positioned at 46 ppm, for the C_α pulses at 56 ppm, and for the carbonyl pulses at 177 ppm. The power of the 90° and 180° $^{13}C_{\alpha/\beta}$ pulses, as well as of the 180° $^{13}C_\alpha$ pulses, is adjusted such that they do not excite the ^{13}CO nuclei (i.e., 4.43, 11.4, 10.6 kHz RF field for 150.9 MHz ^{13}C frequency, respectively). The proton spin-lock pulse, SL, is applied for a duration of 1.8 ms, whereas the carbon $C_{\alpha/\beta}$ spin-lock pulse, SL, is applied for 1 ms at 11.4 kHz. ^{13}C isotropic mixing is accomplished using two cycles of the DIPSI-3 scheme (*13*) (16.1 ms at a field strength of 7 kHz). Delay durations are δ = 1.5 ms, ϵ = 1.05 ms, ζ = 3.2 ms, η = 4.5 ms, θ = 11.4 ms, T_N = 11 ms, κ = 5.4 ms, λ = 2.25 ms. For scheme (A), the initial delays for the t_1 evolution period (see text) were set to t_1^a = 0, t_1^b = 0, t_1^c = 1.05 ms. Increments for those delays were set according to Eq. [2] for a total acquisition time of 6.2 ms. Phase cycling is as follows: $\phi_1 = y$; $\phi_2 = x$, $-x$; $\phi_3 = x$; $\phi_4 = 8(x), 8(y), 8(-x), 8(-y)$; $\phi_5 = 4(x), 4(-x)$; $\phi_6 = 2(x), 2(-x)$; $\phi_7 = 48.5°$ [Bloch–Siegert phase error compensation (*2*)]; $\phi_8 = 4(x), 4(-x)$; $\phi_9 = 8(x), 8(-x)$; $\phi_{10} = 16(x), 16(-x)$; Acq. = $P, -P, -P, P, -P, P, P, -P$, with $P = (x, -x, -x, x)$. Quadrature in the t_1 and t_2 domains is obtained by changing the phases ϕ_3 and ϕ_8, respectively, in the usual States–TPPI manner (*17*). For scheme (B), very weak water presaturation with an ~5 Hz RF field is applied for 800 ms between successive scans. Quadrature in the t_1 domain is obtained by changing the phase ϕ_1 in the States–TPPI manner (*17*). The initial delays for the t_1 components were set to t_1^a = 1.5 ms, t_1^b = 0, t_1^c = 1.5 ms. Increments for those delays were set according to (*2*) for a total acquisition time of 10.1 ms, corresponding to Δt_1^a = 78.7 μs, Δt_1^b = 48.9 μs, Δt_1^c = −22.4 μs.

Between time points c and d, ^{13}C chemical-shift evolution is active for a total time $t_1(\mathrm{CS}) = t_1^a + \epsilon + t_1^b - t_1^c$. ^{1}H–^{13}C J coupling evolution is active for a time $t_1(J_{\mathrm{CH}}) = t_1^a + \epsilon - t_1^b + t_1^c$, J coupling to a carbonyl spin will be active for a time $t_1(J_{CC}) = t_1^a - \epsilon - t_1^b + t_1^c$, and J coupling to another aliphatic carbon is active for $t_1(J_{CC}) = t_1^a + \epsilon + t_1^b + t_1^c$. For optimal performance, it is required that for all t_1 increments $t_1(J_{CC'}) = 0$ and $t_1(J_{\mathrm{CH}}) = \sim 1/(3J_{\mathrm{CH}})$, 2.1 ms in practice

(*10*). In addition, in order to obtain optimal resolution in the F_1 domain of the 3D spectrum, a maximum variation of t_1(CS) is needed for a given maximal duration between time points *c* and *d*. Using arguments similar to those presented elsewhere (*2, 9*), optimal use of the period between time points *c* and *d* is made when the initial durations for the first increment are set to

$$t_1^a(1) = 0 \qquad [1a]$$

$$t_1^b(1) = 0 \qquad [1b]$$

$$t_1^c(1) = \epsilon = 1.05 \text{ ms.} \qquad [1c]$$

For a total number of increments, N, in the t_1 dimension, the increments for t_1^a, t_1^b, and t_1^c are chosen to be

$$\Delta t_1^a = (AT_1/2)/(N-1) \qquad [2a]$$

$$\Delta t_1^b = (AT_1/2 - \epsilon)/(N-1) \qquad [2b]$$

$$\Delta t_1^c = -\epsilon/(N-1), \qquad [2c]$$

where AT_1 is the length of the t_1 acquisition period required for adequate resolution in the F_1 domain of the 3D spectrum. The spectral width in the t_1 dimension, SW_1, is given by

$$SW_1 = (\Delta t_1^a + \Delta t_1^b - \Delta t_1^c)^{-1} \qquad [3]$$

and the size of aliphatic ^{13}C–^{13}C J couplings is scaled by a factor $(AT_1 - 2\epsilon)/AT_1$, increasing the effective resolution.

At time point *d*, a short spin-lock pulse, applied along the ^{13}C x axis, ensures that only terms of the form C_x^β and $C_y^\beta C_z^\alpha$ can be transferred to the C_α spin by the subsequent isotropic mixing period (*11*). Neglecting dephasing caused by $J_{C\alpha C\beta}$ during the short delay 2ϵ, for the first t_1 increment, C_x^β is the only C_β magnetization component present at the beginning of the isotropic mixing period which can result in net transfer to C_α. During isotropic mixing for a duration T, the evolution of this component is described by

$$C_x^\beta \xrightarrow{2\pi J_{C\alpha C\beta} C^\alpha C^\beta T} C_x^\beta[1 + \cos(2\pi J_{C\alpha C\beta}T)]/2 + C_x^\alpha[1 - \cos(2\pi J_{C\alpha C\beta}T)]/2 + C_y^\beta C_z^\alpha[\sin(2\pi J_{C\alpha C\beta}T)] - C_z^\beta C_y^\alpha[\sin(2\pi J_{C\alpha C\beta}T)]. \qquad [4a]$$

Similarly, C_x^α magnetization evolves according to

$$C_x^\alpha \xrightarrow{2\pi J_{C\alpha C\beta} C^\alpha C^\beta T} C_x^\alpha[1 + \cos(2\pi J_{C\alpha C\beta}T)]/2 + C_x^\beta[1 - \cos(2\pi J_{C\alpha C\beta}T)]/2 + C_y^\alpha C_z^\beta[\sin(2\pi J_{C\alpha C\beta}T)] - C_z^\alpha C_y^\beta[\sin(2\pi J_{C\alpha C\beta}T)]. \qquad [4b]$$

As discussed below, not only the second term but also the fourth term on the right-hand side of expression [4a] gives rise to observable magnetization. Similarly, the first and third terms in [4b] contribute to the correlation with C_α. During the delay 2ζ between time points *e* and *f*, rephasing and dephasing of the C_α magnetization takes place due to the weak coupling Hamiltonians $J_{C\alpha C\beta}C_z^\alpha C_z^\beta$ and $J_{C\alpha C'}C_z^\alpha C_z'$, respectively. The two terms of interest evolve according to

$$C_x^\alpha \rightarrow 2C_y^\alpha C_z' \sin(2\pi\zeta J_{C\alpha C'})\cos(2\pi\zeta J_{C\alpha C\beta}) + \cdots \qquad [5a]$$

$$C_z^\beta C_y^\alpha \rightarrow -C_y^\alpha C_z' \sin(2\pi\zeta J_{C\alpha C'}) \times \sin(2\pi\zeta J_{C\alpha C\beta}) + \cdots, \qquad [5b]$$

where $\cdots$ denotes terms that are not transferred into observable magnetization by the remainder of the pulse sequence. Combining the results of expressions [4] and [5] and rearranging the trigonometric terms yield the following transfer functions between time points *c* and *f*:

$$C_x^\alpha \rightarrow C_y^\alpha C_z'\{\cos(2\pi\zeta J_{C\alpha C\beta}) + \cos[2\pi J_{C\alpha C\beta}(\zeta + T)]\}\sin(2\pi\zeta J_{C\alpha C'}) \qquad [6a]$$

$$C_x^\beta \rightarrow C_y^\alpha C_z'\{\cos(2\pi\zeta J_{C\alpha C\beta}) - \cos[2\pi J_{C\alpha C\beta}(\zeta + T)]\}\sin(2\pi\zeta J_{C\alpha C'}). \qquad [6b]$$

$C_y^\alpha C_z'$ terms are transferred into $C_z^\alpha C_y'$ by the 90° pulses applied to $^{13}C_\alpha$ and $^{13}C'$ at time *f*, resulting in $C_y'N_z$ at time *h* (*2*). The 90° $^{13}C'/^{15}N$ pulses, applied at time *h*, convert $C_y'N_z$ into transverse ^{15}N magnetization, which after a constant-time evolution period, of total duration $2T_N$, is converted into transverse amide proton magnetization, observed during the detection period, t_3.

The net magnetization transfer during the pulse sequence from C_α and C_β to H_N for $t_1 = t_2 = 0$ determines the integrated intensity of the C_α–N–H_N and C_β–N–H_N correlations in the C(CO)NH spectra. As can be seen from expression [6], correlations to C_α and C_β can become of opposite sign, de-

FIG. 2. Strip plots of the correlations observed for the amides of residues Gly-121 to Leu-129 of calcineurin B taken from (A) the C(CO)NH and (B) the H(CCO)NH spectrum. Each amide correlates with (A) the aliphatic side-chain carbon resonances of the preceding residue (the preceding residue of Gly-121 is Val-120) and (B) the side-chain protons of the preceding residue. Resonances which are not marked by Greek letters correspond to correlations to amide ^1H–^{15}N pairs that are close in frequency to the one for which the strip has been selected. Solid dots mark C_α, C_β and H_α, H_β correlations that have been observed in 3D CBCA(CO)NH and HBHA(CBCACO)NH spectra (data not shown).

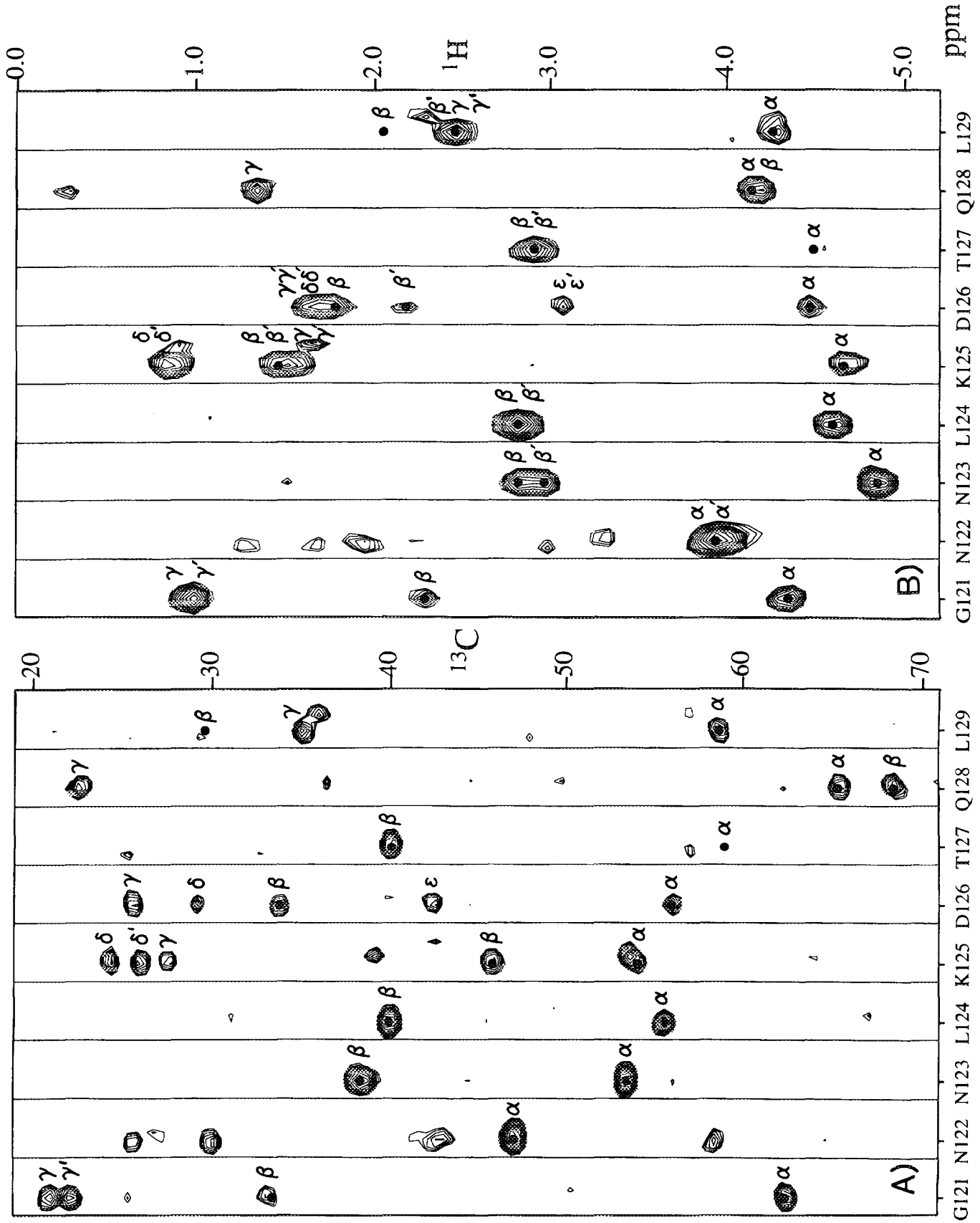
0.0
1.0
2.0
3.0
4.0
5.0
ppm
^{1}H
G121 N122 N123 L124 K125 D126 T127 Q128 L129
B)
20
30
40
50
60
70
^{13}C
G121 N122 N123 L124 K125 D126 T127 Q128 L129
A)

pending on the duration of the isotropic mixing, T, and the value of $J_{C_\alpha C_\beta}$, after scaling for off-resonance effects during isotropic mixing (*7*). This sign reversal is of a different nature than that observed in TOCSY spectra of complex homonuclear spin systems (*12*). In the present case, it results from the fact that the antiphase term, present at the end of the isotropic mixing period, partially refocuses before transfer to another nucleus (cf. Eq. [5b]). As can be seen from expression [6], for a two-spin system this effectively increases the apparent isotropic mixing time by half of the refocusing interval length.

The H(CCO)NH experiment (Fig. 1B) is virtually identical to the C(CO)NH experiment, discussed above. The only difference is found in the position of the t_1 evolution period, which is now inserted between time points *a* and *b*. In order to obtain optimal resolution in the F_1 dimension, the same procedure as that discussed above for the t_1 evolution period in the C(CO)NH experiment is used in the t_1 dimension of the H(CCO)NH experiment. Details are provided in the legend to Fig. 1 and in the description of the HBHA(CBCACO)NH experiment (*2*).

The experiments are demonstrated for a 0.4 ml, 2.3 m*M*, pH 4.9 sample of calcineurin B, a calcium-binding protein of 170 residues (M_r 19.2 kDa), in the presence of 20 m*M* Ca^{2+}. Experiments are carried out on a Bruker AMX-600 spectrometer, operating at 37°C, equipped with an external class A/B 100 W power amplifier for the ^{13}C channel, and using Software Version 920501. A data matrix of 57* × 32* × 512* data points, where *n** refers to *n* complex data points, was used for the C(CO)NH experiment and 68* × 32* × 512* data points for the H(CCO)NH data set. Acquisition times were 6.2 ms (t_1), 19.8 ms (t_2), and 55.3 ms (t_3) for the C(CO)NH experiment and 10.1 ms (t_1), 19.8 ms (t_2), and 55.3 ms (t_3) for the H(CCO)NH experiment. Spectra were acquired using a 32-step phase cycle, repeated four times for each t_1 and t_2 increment to obtain quadrature information in these dimensions. The total measuring times were 77 and 87 h for the C(CO)NH and H(CCO)NH data sets, respectively. Further details regarding the experiment are given in the legend to Fig. 1. For both data sets, after digital filtering with a 60°-shifted sine-bell function in the t_1 and t_3 dimensions, zero filling to 128* (t_1) and 1024* (t_3), and Fourier transformation, the length of the t_2 time domain was doubled by mirror image linear prediction (*14*), prior to cosine-squared windowing, zero filling to 128*, and Fourier transformation.

Figure 2A shows strips from the 3D C(CO)NH spectrum, taken parallel to the F_1 axis, for the amides of residues Gly-121 through Leu-129. Each amide shows the J correlations to the carbons of the side chain of the preceding residue. Solid dots mark the positions of C_α and C_β resonances observed in the CBCA(CO)NH spectrum (data not shown). For the 16 ms isotropic mixing time used, the correlations with many of the C_α and C_β resonances are much weaker than those to C_γ and C_δ resonances. Thus, the previously described CBCA(CO)NH experiment clearly provides a useful complement to the C(CO)NH data. The present data are particularly useful as they indicate immediately the residue type for many of the residues with long side chains.

Figure 2B shows F_1 strips from the 3D H(CCO)NH spectrum, for the same amides as those shown in Fig. 2A. These strips now show correlations to the protons of the side chain preceding the observed amide. Again, solid dots mark the positions of H_α and H_β resonances, observed in the HBHA(CBCACO)NH spectrum (data not shown). With few exceptions, it is readily clear from inspection of Figs. 2A and 2B which of the side-chain proton resonances corresponds to which side-chain carbon resonance. This avoids the need for recording a 4D HC(CO)NH spectrum, in which the ^1H and ^{13}C frequencies of the side chains are measured simultaneously, albeit at much lower frequency resolution.

The experiments described above provide an extremely convenient method for obtaining a majority of the ^1H and ^{13}C side-chain assignments by linking them directly to the backbone amide resonances, which typically show a much lower degree of spectral overlap than the C_α/H_α resonances. The C(CO)NH and H(CCO)NH experiments are significantly lower in sensitivity than, for example, the CBCA(CO)NH experiment, mainly because of the relaxation occurring during the isotropic mixing and because of the fact that only a fraction of the side-chain ^{13}C magnetization is transferred to C_α by the isotropic mixing, prior to relay to the observed amide. Nevertheless, as demonstrated here, the experiment is applicable to proteins with sizes of up to 20 kDa, provided the sample concentration is at least several millimolar. As shown for the HCCH–TOCSY experiment, the intensities of the correlations are rather complex functions of the side-chain topology, the scaling of the J_{CC} couplings caused by finite RF power, and the duration of the mixing period (*15, 16*). As discussed above, the intensity of magnetization transfer from side-chain carbons to C_α follows a time dependence which is quite similar to that observed in the HCCH–TOCSY experiment, with the main difference that the curves derived previously are shifted to shorter mixing times by a few milliseconds, because of the refocusing of antiphase $C_y^\alpha C_z^\beta$ terms during the delay 2ζ.

ACKNOWLEDGMENTS

We thank Claude Klee for help and encouragement in our study of calcineurin B, Hao Ren for protein expression, and Marius Clore and Dennis Torchia for useful discussions. This work was supported by the AIDS Targeted Anti-Viral Program of the Office of the Director of the National Institutes of Health.

REFERENCES

1. S. Grzesiek and A. Bax, *J. Am. Chem. Soc.* **114**, 6291 (1992).
2. S. Grzesiek and A. Bax, *J. Biomol. NMR*, in press.

3. S. Grzesiek and A. Bax, *J. Magn. Reson.* **99,** 201 (1992).
4. L. E. Kay, M. Ikura, and A. Bax, *J. Am. Chem. Soc.* **112,** 888 (1990).
5. A. Bax, G. M. Clore, P. C. Driscoll, A. M. Gronenborn, M. Ikura, and L. E. Kay, *J. Magn. Reson.* **87,** 620 (1990).
6. S. W. Fesik, H. L. Eaton, E. T. Olejniczak, E. R. P. Zuiderweg, L. P. McIntosh, and F. W. Dahlquist, *J. Am. Chem. Soc.* **112,** 886 (1990).
7. A. Bax, G. M. Clore, and A. M. Gronenborn, *J. Magn. Reson.* **88,** 425 (1990).
8. B. A. Messerle, G. Wider, G. Otting, C. Weber, and K. Wüthrich, *J. Magn. Reson.* **85,** 608 (1989).
9. T. D. Spitzer, G. E. Martin, R. C. Crouch, J. P. Shockcor, and B. T. Farmer II, *J. Magn. Reson.* **99,** 433 (1989).
10. D. P. Burum and R. R. Ernst, *J. Magn. Reson.* **39,** 163 (1980).
11. A. Bax and D. G. Davis, *J. Magn. Reson.* **65,** 355 (1985).
12. M. Rance, *Chem. Phys. Lett.* **154,** 242–247 (1989).
13. A. J. Shaka, C. J. Lee, and A. Pines, *J. Magn. Reson.* **77,** 274 (1988).
14. G. Zhu and A. Bax, *J. Magn. Reson.* **90,** 405 (1990).
15. H. L. Eaton, S. W. Fesik, S. J. Glaser, and G. P. Drobny, *J. Magn. Reson.* **90,** 452 (1990).
16. G. M. Clore, A. Bax, P. C. Driscoll, P. T. Wingfield, and A. M. Gronenborn, *Biochemistry* **29,** 8172 (1990).
17. D. Marion, M. Ikura, R. Tschudin, and A. Bax, *J. Magn. Reson.* **85,** 393 (1989).